Production of Carbon Nanotubes in a Packed Bed and a Fluidized Bed

Qian Weizhong, Wei Fei, Wang Zhanwen, Liu Tang, Yu Hao, Luo Guohua, and Xiang Lan
Dept. of Chemical Engineering, Tsinghua University, Beijing, 100084, China

Deng Xiangyi
Dept. of Chemistry, Huangshi College, Huangshi, Hubei, 435002, China

Carbon nanotubes (CNTs) prepared from ethylene decomposition over the Fe/Al_2O_3 catalyst are studied in a packed bed (PB) reactor and a nanoagglomerate fluidized bed reactor (NABR), respectively. CNTs sampled at different reaction times are characterized by TEM, Raman spectroscopy, and particle size analysis. The bulk density and agglomerate size of CNTs increase significantly with reaction time in a PB, while it remains at a stable level in NABR. Also, CNTs with good morphology, narrow diameter distribution, and fewer lattice defects are obtained in an NABR, rather than in a PB. In contrast to the unavoidable jamming due to volume increase of CNTs observed in a PB, a continuous CNT growth process is attained in an NABR, even though the amount of CNTs in an NABR is 6−7 times that in a PB. The flow dynamics, available space for growing, and mass and heat transfer can be controlled in an NABR, which favors the large-scale production of CNTs with uniform properties.

Introduction

Since the discovery of carbon nanotubes (CNTs) in 1991 (Iijima, 1991), its preparation and application has been widely studied. However, due to difficulties in the preparation of single-walled nanotubes and in the scale-up production of multiwalled nanotubes (Krijn and John, 2000), many of these studies were based on small amounts of CNTs, and this has to some degree influenced the progress of research and the accuracy of experimental data giving rise to some controversy, such as in the study of hydrogen adsorption (Tibbetts et al., 2001). The large-scale preparation of CNTs is necessary for further fundamental research and its ultimate application, and the commercialization of CNTs. Catalytic chemical vapor deposition is a promising method for the large-scale production of CNTs (Krijn and John, 2000). In most cases, the process is conducted in a gas-solid system. The volume of the solid phase increases during the process as carbon gradually deposits on the catalyst. The control of temperature, pressure drop, and mass and heat transfer are important for producing large amounts of CNTs of uniform quality. The packed-bed reactor was widely adopted in previous studies (Zhang and Amiridis, 1998; Li et al., 2000) due to its simplicity. The catalyst and CNTs remain fixed under a relatively small superficial gas velocity in the packed-bed reactor. However, CNTs are solid products and the solid volume steadily increase, which is different from the traditional packed-bed reactor used in other catalytic processes. Limited space for growth may lead to an uncontrollable jam of the reactor during the reaction (Zhang and Amiridis, 1998; Krijn and John, 2000; Li et al., 2000), which can become serious in the large-scale production of CNTs. Reactors in which the transport of the solid materials can be carried out easily are proposed to solve the problem. These include a reactor adopted in a floating catalyst method (Ci et al., 1999; Ting et al., 1999) and fluidized-bed reactors (Hernadi et al., 1996; Meier et al., 1998; Qian et al., 2001). In the former reactors, the CNTs are prepared in a very dilute solid phase, and the yield of CNTs is relatively low when compared to the scale of the reactor. Also, the CNTs pass through the reactor with very short residence times that are insufficient for the full use of the activity of the catalyst. In the latter fluidized-bed reactor, the residence

Correspondence concerning this article should be addressed to W. Fei.

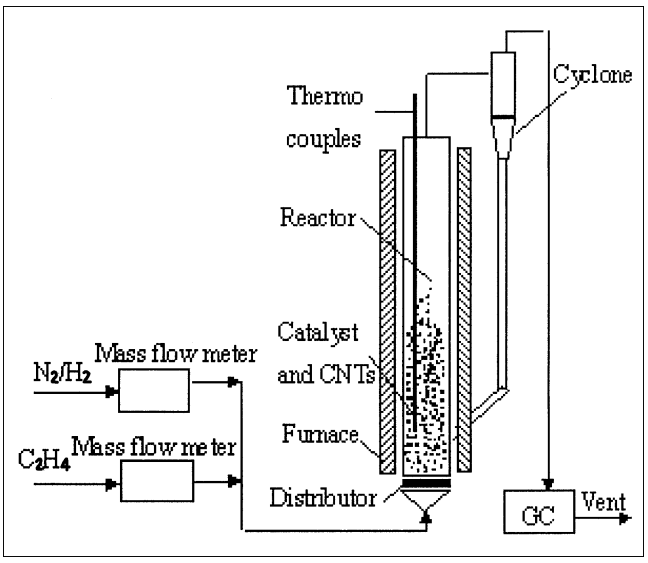

Figure 1. Reaction system.

times of the CNTs can be controlled accurately and the activity of the catalyst is utilized sufficiently to achieve high yields of CNTs, which is important for large-scale production since the catalyst is expensive. Furthermore, heat and mass transfer is good in a fluidized bed, which is important for the stable growth of CNTs. However, in previous studies (Hernadi et al., 1996; Meier et al., 1998; Qian et al., 2001), the amount of CNTs produced was too small for the understanding of the collective behavior of CNTs in large quantities. In this contribution, a 10 g catalyst is used to produce 30–150 g CNTs, which is enough to evaluate the effect of the hydrodynamics in a packed-bed reactor and a nanoagglomerate fluidized-bed reactor (Wei et al., 2001) on the growth of CNTs. Changing properties of the CNTs with reaction time including micromorphology, lattice defects, diameter distribution, bulk density, and particle-size distribution of its agglomerates are studied in a packed-bed reactor and a nanoagglomerate fluidized-bed reactor, respectively, which is important for the controlled production of CNTs in a large scale.

Experimental Studies

The Fe/Al_2O_3 catalyst is prepared by a co-precipitation method. Most of the iron crystallines on the catalyst are smaller than 15 nm. The average size of the catalyst particle agglomerates is about 50 μm. The carbon source is ethylene. 2 mol hydrogen and heat of 52.26 KJ/mol in the exothermic reaction are produced from the decomposition of 1 mol ethylene. The reaction system is shown in Figure 1. The reactor is made of stainless steel with an inner dia. of 40 mm and a height of 1,000 mm. To make CNTs, 10 g catalyst is packed into the reactor and is first reduced by hydrogen at 823 K for 2 h. A mixture of nitrogen and ethylene of 99.99% purity is then fed into the reactor and decomposed at 823 K. The volume ratio of nitrogen to ethylene is 2:3. An online gas chromatography (HP4890D) is used to detect gas products. The conversion of ethylene and the yield of CNTs at different times are obtained from the gas analysis.

In the operation of the packed-bed reactor, the gas velocity is controlled at 0.01 m/s. The catalyst and CNTs remain fixed in the reactor during the entire reaction period. When the reaction time reaches the desired value, the ethylene is shut off and nitrogen is introduced into the reactor to cool the CNTs products. CNTs samples are then collected. In the operation of the nanoagglomerate fluidized-bed reactor (Wei et al., 2001), the gas velocity is 0.1 m/s. CNTs growing on the catalyst exist as nanoagglomerates, which can be fluidized smoothly by the gaseous reactants (Brooks and Fitzsgerald, 1985; Wang et al., 2002). After specified intervals of time, small amounts of a CNT sample (2–4 mL) are taken through the sample device. Since the fluidization is uniform in the NABR, the sampled CNT products are assumed the same as in the rest of the reactor. Thus, samples taken at different times can reveal changes in the properties of the CNTs during their growth process.

All samples are characterized by Raman spectroscopy (Renishaw, RM2000, excited at 514.5 nm) and Transmission Electron Microscopy (TEM, Hitachi-800). The diameter distribution of individual CNT is obtained from the measurement of the diameters of nearly 1,600 individual tubes in 20 TEM pictures of the samples from the different reactors, respectively. The particle-size distribution of CNT agglomerates is measured using a Malvern Mastersizer (Mastersizer 2.5, 0.05–555 μm). The bulk density of the CNTs is determined from its volume and weight.

Result and Discussion

The conversion of ethylene in different reactors is shown in Figure 2. The conversion of ethylene is above 95% in the packed-bed reactor during the entire reaction period. The conversion of ethylene is maintained at 100% at the beginning, then decreases after 45 min., and finally is 50% after 307 min in the NABR. The space velocity of ethylene in the nanoagglomerate fluidized-bed reactor is 10 times higher than that in the packed-bed reactor. Catalyst deactivation (Bartholomew, 2001) and a high space velocity make conversion of the ethylene decrease linearly with reaction time. Figure 3 shows the yield of CNTs per unit catalyst in the nanoagglomerate fluidized-bed reactor and packed-bed reactor. The yield of CNTs increases steadily with the reaction time in both reactors. The total yield of CNTs in the nanoag-

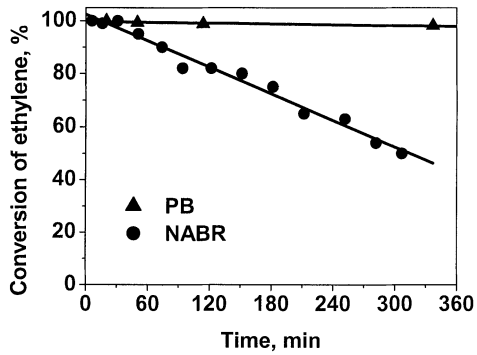

Figure 2. Conversion of ethylene with reaction time in the PB and the NABR.

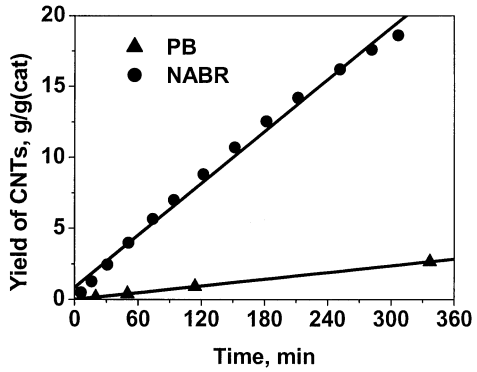

Figure 3. Yield of CNTs with reaction time in the PB and the NABR.

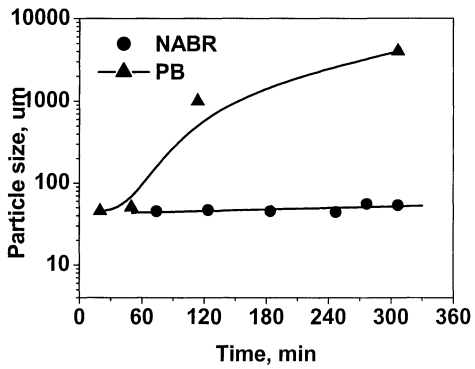

Figure 5. Variation of the average CNT agglomerate size with reaction time in the PB and the NABR.

glomerate fluidized-bed reactor is 6–7 times that in the packed-bed reactor at the end of reaction, due to the ten-fold increase of the space velocity in the nanoagglomerate fluidized-bed reactor.

When a large amount of CNTs is produced, the packing density and particle size of its nanoagglomerate can be measured. The bulk density of CNT samples after different reaction times is shown in Figure 4. At the beginning of the reaction period, the bulk density of the CNTs is nearly equal to that of the catalyst. In the following period of 6–100 min., it decreases gradually as carbon is deposited on the catalyst. This tendency is observed in both reactors, indicating that the amount of CNTs is small in the initial stage of CNT growth and the growing space is large enough even in the packed-bed reactor. However, when the amount of CNTs is large enough, the hydrodynamics of the gas and solid in the reactors will exert an influence on the bulk density of the CNTs. In the packed-bed reactor, the CNTs are unable to move and entangled CNTs tend to pile up more and more tightly, as shown in Figure 4. Its bulk density will increase with reaction time. However, the CNTs can move and the growth is not hindered in the nanoagglomerate fluidized-bed reactor. With an increasing carbon deposition on the catalyst, its bulk density decreases steadily to 75–100 kg/m^3.

According to the work of Brooks et al. (Brooks and Fitzsgerald, 1985) and Wang et al. (2002), nanometer particles tend to form agglomerates of 20–500 μm. These agglomerates have different behaviors in different reactors with different hydrodynamic states. The average particle size of CNT agglomerates with reaction time in the different reactors is shown in Figure 5. The particle size of CNT agglomerates in the packed-bed reactor increases significantly with reaction time after 50 min. The average size of the CNT agglomerates is 1 mm at 114 min. and about 4 mm at 337 min., respectively. When CNTs grow, they grow out from the catalyst support in a scattered direction. The tubes will entangle each other and form large agglomerate particles, which grow larger in a packed-bed reactor with a steady increase in its density. It is noted that the yield of CNTs in the packed-bed reactor is less than two-fold the catalyst weight, which indicates that the flow dynamics has a significant influence on the agglomerate of CNTs. However, as shown in Figures 5 and 6, the particle size of CNT agglomerates in the nanoagglomerate fluidized-bed reactor remains unchanged with an increasing reaction time. Individual CNTs can grow freely and are less influenced by other tubes in the nanoagglomerate fluidized-bed reactor. It is noted that average particle size of CNT agglomerate in nanoagglomerate fluidized-bed reactor remains at 45–50 μm. It is close to the size of particle type A in the Geldart classification, which has very good fluidization properties. Combining the results of the bulk density in Figure 4, it is clear that CNTs growth in a fluidized state is a rather

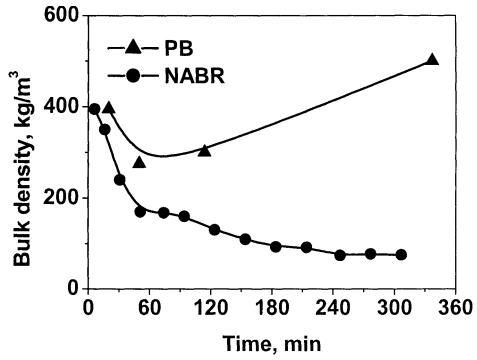

Figure 4. Bulk density of CNT agglomerates with reaction time in the PB and the NABR.

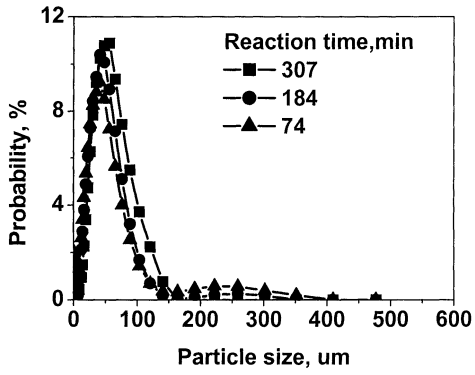

Figure 6. CNT agglomerate size distribution in the NABR at different reaction times.

uniform process, which favors the control of its synthesis in large scale.

Jamming of the reactor occurs in the packed-bed reactor at 337 min due to the significant solid volume increase by the CNTs. Cross-linked CNT agglomerates form the bulk of the solids with a significant increase in the pressure drop in the reactor. A batch operation has to be adopted, although the catalysts still have enough activity to crack ethylene, and leads to a time-consuming and low efficiency process. However, even though the yield of CNTs in the nanoagglomerate fluidized-bed reactor at 307 min is 6–7 times that in the packed-bed reactor at 337 min, a continuous operation is attained in the nanoagglomerate fluidized-bed reactor. First, fluidized CNTs can grow freely in the sufficient space made available. Secondly, the placement of a catalyst container and a CNTs collector at a selected place in the nanoagglomerate fluidized-bed reactor will allow the catalyst to be sent into the reactor, and CNTs products can be transferred out of the reactor when the volume of CNTs is relatively large or when CNT growth ceases due to deactivation of the catalyst. It is clear that the nanoagglomerate fluidized-bed reactor proposed in this article can allow the large-scale continuous production of CNTs.

The microstructure of the CNTs and its morphology are observed by TEM. Samples collected at different times in the nanoagglomerate fluidized-bed reactor and the packed-bed reactor are shown in Figures 7 and 8, respectively. Like much previous work on the preparation of CNTs via the CVD method (Baker, 1989; Hernadi et al., 1996; Meier et al., 1998; Zhang and Amiridis, 1998; Krijn and John, 2000; Li et al., 2000; Qian et al., 2001), in this article ethylene is continually cracked over an iron-based catalyst to produce carbon and hydrogen. Carbon gradually accumulates on the catalyst in an ordered structure to form CNTs. Detachment of iron particles from the support (Al_2O_3) due to carbon accumulation is generally observed. Iron particles in the nanometer range are found in the tip of the CNTs. Also, the diameter of the CNTs depends on the crystalline size of the metal particles at its tip (Baker, 1989; Hernadi et al., 1996; Krijn and John, 2000). For the CNTs prepared from the nanoagglomerate fluidized-bed reactor, no obvious differences are observed in the samples at different reaction times (Figures 7a and 7b). The morphology of these tubes is fairly good. They are all very long and have the same diameter. Less soot and amorphous carbon are found in the samples. It suggests that the morphology of the CNTs is uniform in the nanoagglomerate fluidized-bed reactor. However, obvious differences in the morphology of the CNTs from the packed-bed reactor at different times exist (Figures 8a and 8b). More black parts, soot, and broken tubes are observed in the CNTs sample at 50 min. Relatively long tubes tending to form large agglomerates are observed in the packed-bed reactor at 337 min. Comparing Figures 7

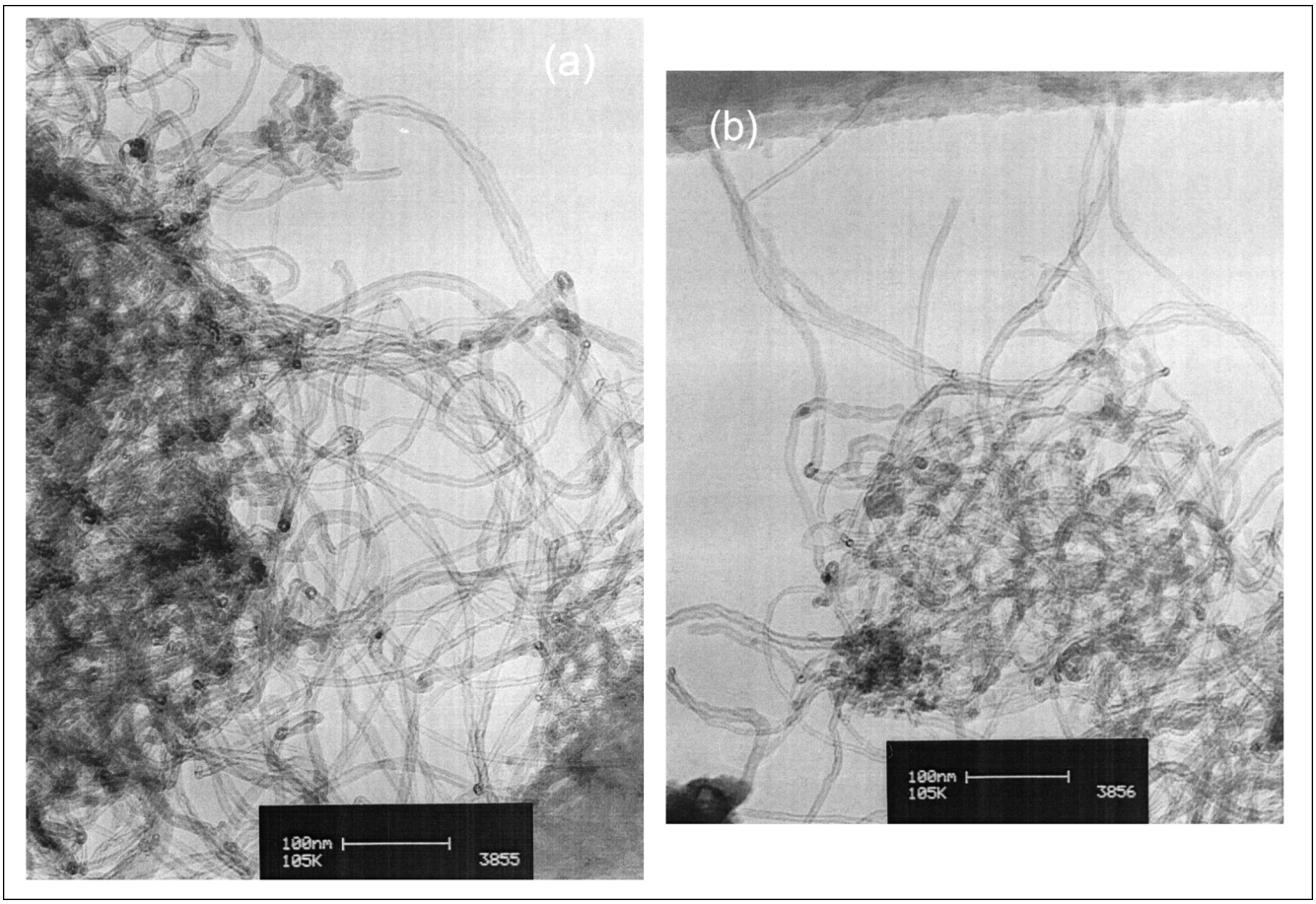

Figure 7. TEM image of CNTs in the NABR (a: 124 min, B; 307 min).

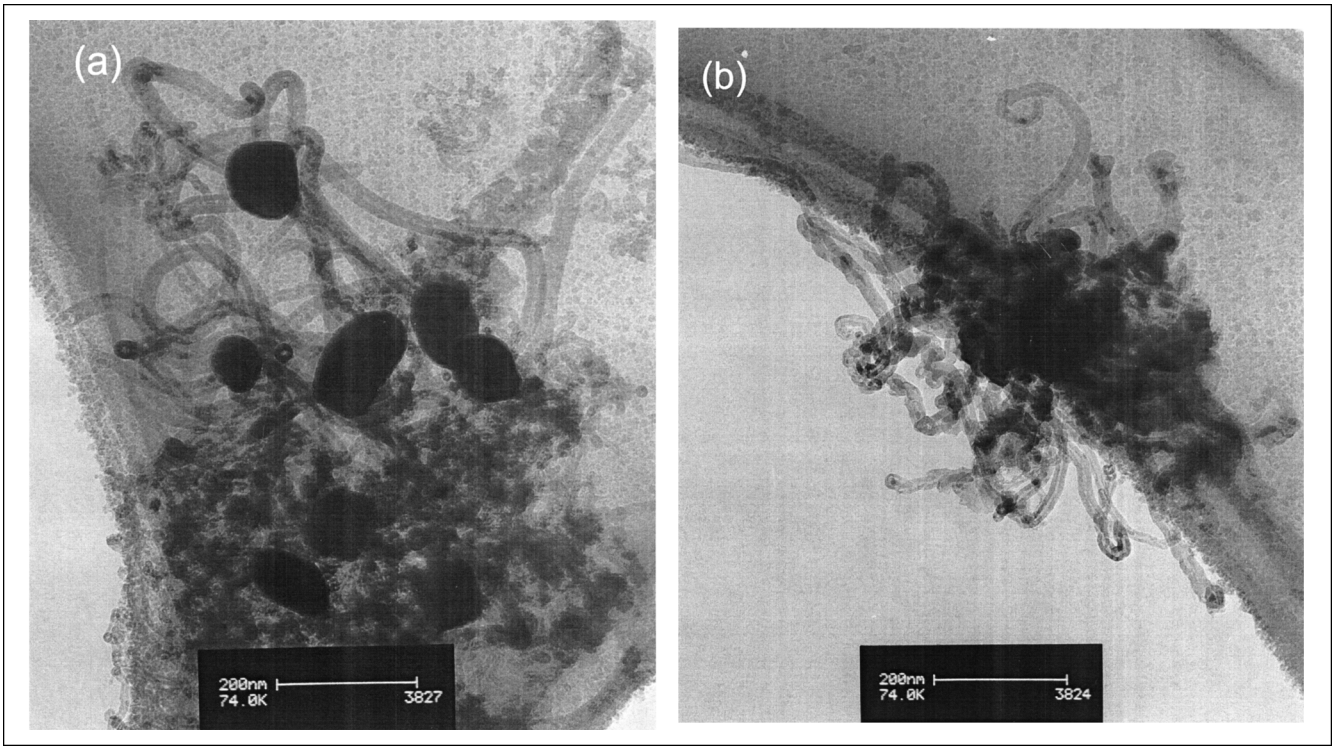

Figure 8. TEM image of CNTs in the PB (a: 50 min, B: 337 min).

and 8, the tubes in the nanoagglomerate fluidized-bed reactor are obviously longer than in the packed-bed reactor. The detailed diameter distribution of the individual CNTs is shown in Figure 9. The diameter distribution of CNTs from the nanoagglomerate fluidized-bed reactor is very narrow and most of tubes are in the range of 3–16 nm with an average diameter of 8 nm. However, the diameter distribution of CNTs from the packed-bed reactor is relatively wide. Nearly 30% of the CNTs from the packed-bed reactor are larger than 16 nm. The average diameter of the CNTs from the packed-bed reactor is 16 nm. Since a catalyst with the same nanometer crystalline size distribution is used in both reactors and the diameter of CNTs depends on the metal crystalline size on the catalyst, the diameter distribution of the CNTs reflects the dispersion of the catalyst particles in different reactors directly. For CNTs prepared in the packed-bed reactor, the catalyst particles and the as-grown CNTs are unable to move and are packed relatively tightly in the packed-bed reactor. It is possible, as observed in many packed-bed reactors (Smith, 1973), that heat transfer in the packed-bed reactor is relatively poor due to diffusion resistance inside the bulk catalyst particle, which will become even worse with an increase of the CNT agglomerate size. Therefore, when the reaction heat is produced from ethylene decomposition, the heat inside the CNT or catalyst agglomerates cannot be transferred out effectively and the temperature inside the agglomerate will be higher than that of the bulk gas phase. This may cause sintering and size increase of metal particles on the catalyst (Bartholomew, 2001), which may be the reason why nearly 30% of the CNTs from the packed-bed reactor are 20–40 nm. However, the fluidized state of the gas and solid in the nanoagglomerate fluidized-bed reactor allows good heat transfer between the CNT agglomerates and the bulk gas phase in the nanoagglomerate fluidized-bed reactor and there will not be any metal particle size increase as in the packed-bed reactor. Furthermore, the size of the catalyst agglomerates can be still smaller due to the freedom for continuous stretching of the CNTs from the catalyst particle out to a relatively large and free space in the nanoagglomerate fluidized-bed reactor. These factors altogether lead to the narrow diameter distribution and long length of the individual CNTs in the nanoagglomerate fluidized-bed reactor.

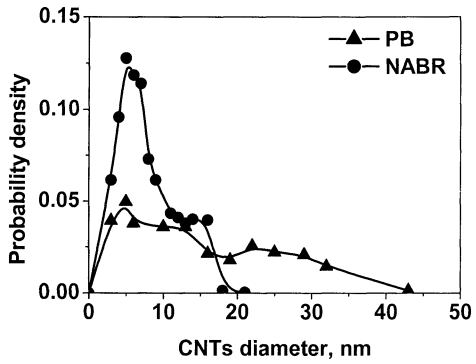

Figure 9. Outer diameter distribution of the CNTs in the PB and the NABR.

Raman spectroscopy is used to study changes in the microstructure of the CNTs after different growth periods in the reactors. Since Raman spectroscopy can probe samples

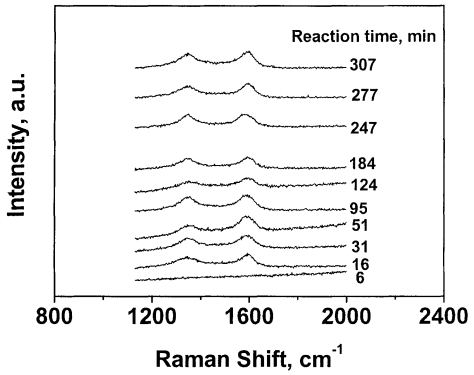

Figure 10. Raman Spectra of CNTs at different reaction times in the NABR.

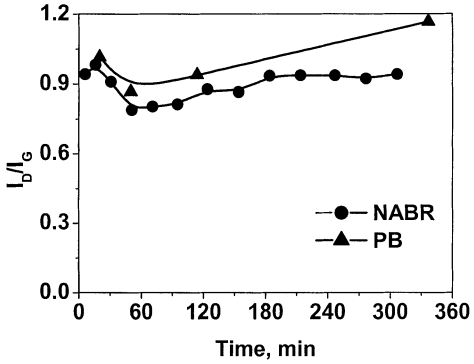

Figure 12. Variation of the intensity ratio of the D line to G line in the Raman spectrum of the CNTs with reaction times in the PB and the NABR.

larger than 10–50 μm and thicker than 0.5 μm, it is a more convenient technique than TEM to detect the changes occurring during the growth of CNTs on a relatively large scale. Generally, in the Raman spectrum, the ordered graphite structure has a strong peak centered at 1,570–1,610 cm^{-1}, which is called the G line (Dresselhaus et al., 2000), and the disordered structure or lattice defects has a strong peak centered at $\sim$1,340 cm^{-1}, which is called the D line. The Raman spectra of samples at different reaction times in the nanoagglomerate fluidized-bed reactor are shown in Figure 10. No obvious peak is found at the beginning of the reaction period, after which the intensity and width of the D line and G line remain the same in the reaction time period from 16 min to 307 min. These results indicate that the growth of CNTs in the nanoagglomerate fluidized-bed reactor is a uniform process and the microstructures of the CNTs are very stable. However, as shown in Figure 11, the samples at different reaction times in the packed-bed reactor show significant fluctuations in the intensity and width of the D line and G line, which implies that the change in the macroscopic properties of the CNTs in the packed-bed reactor described above influence the microstructure of the CNTs. Generally, the intensity ratio (R) of the D line to G line is used to evaluate the defects of CNTs (Dresselhaus et al., 2000). Relatively lower values of R mean less defects and higher quality CNTs. The ratios of R after different reaction times in the different reactors are shown in Figure 12. The value of R in the nanoagglomerate fluidized-bed reactor is always lower than that in the packed-bed reactor during the entire reaction period. It is clear that defects in the CNTs are not increased by the relatively more turbulent contact of gas and CNTs, but actually decreased to some degree due to the presence of sufficient growing space and fairly uniform temperatures in the nanoagglomerate fluidized-bed reactor. As shown in Figure 12, an obvious decrease in this ratio is observed in the initial growth period (about 50 min) in both reactors, which suggests that some time is needed for the carbon to deposit in a relatively good structure. In the following reaction period from 50 min to 300 min, the value of R does not change with the increasing reaction time in the nanoagglomerate fluidized-bed reactor. However, the value of R in the packed-bed reactor increases with reaction time, which shows that defects in the CNTs increase with the significant change in its bulk density shown in Figure 4. The change in the intensity ratio (R) of the Raman spectra is in agreement with the change in the bulk density in both reactors. The available growing space for CNTs inside the agglomerates will become less and less in the packed-bed reactor, and more distorted or broken tubes will be produced due to this space limitation in the packed-bed reactor. These tubes have serious lattice defects, which are reflected in the peak at $\sim$1,340 cm^{-1} in the Raman spectrum. In contrast, the availability of sufficient growing space in the nanoagglomerate fluidized-bed reactor leads to fewer defects in the CNTs. It is clear that the microstructure of the CNTs strongly depends on the hydrodynamic state in the reactor.

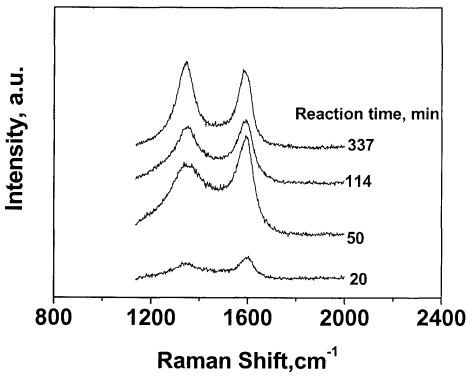

Figure 11. Raman Spectra of the CNTs at different times in the PB.

The above comparison of CNTs produced in the two different reactors indicates that the preparation of uniform CNTs can be realized in the nanoagglomerate fluidized-bed reactor based on CNT agglomerate fluidization. Due to the controlled flow dynamics, available space, and efficient heat and mass transfer in the nanoagglomerate fluidized-bed reactor, large amounts of CNTs with fairly well structured morphology, less lattice defects, and stable macroscopic properties are obtained. This is different from the results of Hernadi et al. obtained with a fluidized-bed reactor (Hernadi et al., 1996) where the size of the reactor is very small. Possibly, during the growth of CNTs in their reactor, there is more opportunity for the CNTs to contact with the reactor wall

than is the case in the large size nanoagglomerate fluidized-bed reactor in this article. The negative effect of the reactor wall on the growth of CNTs may be serious. Therefore, soot and broken CNTs were observed in their work. It is also shown that the growth of CNTs can be influenced by many factors, and the design of the reactor is an important consideration in the growth of CNTs. The synthesis of CNTs in a relatively large reactor, while 200 mm inner dia. is underway.

Conclusion

The same catalyst was used to study the large-scale growth of CNTs in different types of reactors. A nanoagglomerate fluidized-bed reactor has the advantages of good mass and heat transfer, and provides a uniform temperature condition and a relatively large space for the growth of fluidized CNTs. The macroscopic properties including bulk density and particle size of the CNT agglomerates remain stable during the entire reaction period. However, significant changes in the bulk density and particle size of the CNT agglomerates are observed in the packed-bed reactor with reaction time. Furthermore, the nanoagglomerates fluidized-bed reactor can perform well even after the volume and yield of CNTs is 6–7 times that in the packed-bed reactor. Jamming of the reactor is observed in the packed-bed reactor at 337 min due to the volume increase of the solid phase by the CNTs. TEM characterization shows that individual CNTs with fairly good morphology and a narrower diameter distribution is obtained in the nanoagglomerate fluidized-bed reactor in comparison with the packed-bed reactor. The use of the intensity ratio of the D line to G line in the Raman spectra of the CNTs indicates that fewer defects are present in the CNTs obtained from the nanoagglomerate fluidized-bed reactor. The changes in the microstructure of the CNTs are in agreement with the changes in the macroscopic properties including the bulk density and particle size of the CNT agglomerates. From the above comparison of CNTs prepared in large quantities in the different reactors, it is seen that the dispersion on the catalyst, the morphology of the CNTs, the diameter distribution of the CNTs, and the microscopic stack structure and macroscopic packing state of the CNTs strongly depends on the characteristics of the reactors. The nanoagglomerate fluidized-bed reactor adopted in this article allows the controlled large-scale preparation of CNTs with uniform properties.

Acknowledgments

This work was supported by the Natural Science Foundation of China (No.20006009).

Literature Cited

Baker, R. T. K., "Catalytic Growth of Carbon Filaments," *Carbon*, **27**, 315 (1989).

Bartholomew, C. H., "Mechanism of Catalyst Deactivation," *Appl. Catal. A: General*, **212**, 17 (2001).

Brooks, E. F., and T. J. Fitzsgerald, "Aggregation and Fluidization Characteristics of a Fibrous Carbon," AIChE Meeting, New York, 21 (1985).

Ci, L. J., B. Q. Wei, L. Ji, C. L. Xu, and D. H. Wu, "Preparation of Carbon Nanotubules by the Floating Catalyst Method," *J. of Mat. Sci. Lett.*, **18**, 797 (1999).

Dresselhaus, M. S., M. A. Pimenta, P. C. Eklund, and G. Dresselhaus, "Raman Scattering in Fullerenes and Related Carbon-Based Materials," *Raman Scattering in Materials Science*, W. H. Weber and R. Merlin, eds., Springer, Berlin, p. 314 (2000).

Hernadi, K., A. Fonseca, J. B. Nagy, D. Bernaerts, and A. A. Luca, "Fe-Catalyzed Carbon Nanotube Formations," *Carbon*, **34**, 1249 (1996).

Iijima, S., "Helical Microtubules of Graphitic Carbon," *Nature*, **354**, 56 (1991).

Krijn, P. D. J., and W. G. John, "Carbon Nanofibers: Catalytic Synthesis and Applications," *Catal. Rev.: Sci. and Eng.*, **42**, 481 (2000).

Li, Y. D., J. L. Chen, Y. N. Qin, and C. Liu, "Simultaneous Production of Hydrogen and Nanocarbon from Decomposition of Methane on a Nickel-Based Catalyst," *Energy & Fuels*, **141**, 188 (2000).

Meier, A., V. A. Kirillov, G. G. Kuvshinov, Yu. I. Mogilnykh, A. Weidenkaff, and A. Steinfeld, "Production of Catalytic Filamentous Carbon by Solar Thermal Decomposition of Hydrocarbons," *J. De Physique. IV: JP*, **9**, 393 (1998).

Qian, W. Z., Z. W. Wang, F. Wei, Y. Jin, Y. D. Li, T. Liu, and J. C. Li, "Production of Carbon Nanotubes from Methane Decomposition over Nickel Catalyst in Fluidized Bed Reactor," Int. Catalysis Workshop for Young Scientists, Beijing, p. 319 (Sept. 2001).

Smith, J. M., "Interpretative Review Heat Transfer in Packed-Bed Reactors," *Chem. Eng. J. and Biochem. Eng. J.*, **2**, 109 (1973),

Tibbetts, G. G., G. P. Meisner, and C. H. Olk, "Hydrogen Storage Capacity of Carbon Nanotubes, Filaments, and Vapor-Grown Fibers," *Carbon*, **39**, 2291 (2001).

Ting, M. J., N. Z. Huang, and B. C. L. Jones, "TEM Observation of Carbon Tubes Produced by a Continuous Process," *J. of Mat. Sci.*, **34**, 5233 (1999).

Wang, Y., G. S. Gu, F. Wei, and J. Wu, "Fluidization and Agglomerate Structure of SiO_2 Nanoparticles," *Powder Technol.*, **124**, 152 (2002).

Wei, F., G. H. Luo, Y. Wang, Z. F. Li, Z. W. Wang, W. Z. Qian, and Y. Jin, "A Method and a Fluidized Bed Reactor for Continuous Production of CNTs," Patent No. CN 01118349.7 (2001).

Zhang, T. J. and M. D. Amiridis, "Hydrogen Production via the Direct Cracking of Methane over Silica-Supported Nickel Catalysts," *Appl. Catal. A: General*, **167**, 161 (1998).

Manuscript received Feb. 13, 2002, and revision received Sept. 18, 2002.